

The short term climatic sensitivity of carbonate and silicate weathering fluxes: Insight from seasonal variations in river chemistry

Edward T. Tipper^{a,*}, Mike J. Bickle^a, Albert Galy^a, A. Joshua West^b,
Catherine Pomiès^a, Hazel J. Chapman^a

^a Department of Earth Sciences, University of Cambridge, Downing Street, Cambridge CB2 3EQ, UK

^b Department of Earth Sciences, University of Oxford, Parks Road, Oxford OX4 1EW, UK

Received 15 November 2005; accepted in revised form 13 March 2006

Abstract

Large seasonal variations in the dissolved load of the headwater tributaries of the Marsyandi river (Nepal Himalaya) for major cations and ⁸⁷Sr/⁸⁶Sr ratios are interpreted to result from a greater dissolution of carbonate relative to silicate at high runoff. There is up to a 0.003 decrease in strontium isotope ratios and a factor of 3 reduction in the Si(OH)₄/Ca ratio during the monsoon. These variations, in small rivers sampling uniform lithologies, result from a different response of carbonate and silicate mineral dissolution to climatic forcing. Similar trends are observed in compiled literature data, from both Indian and Nepalese Himalayan rivers. Carbonate weathering is more sensitive to monsoonal runoff because of its faster dissolution kinetics. Silicate weathering increases relative to carbonate during the dry season, and may be more predominant in groundwater with longer water–rock interaction times. Despite this kinetic effect, silicate weathering fluxes are dominated by the monsoon flux, when between 50% and 70% of total annual silicate weathering flux occurs.

© 2006 Elsevier Inc. All rights reserved.

1. Introduction

The removal of atmospheric CO₂ by weathering of silicate minerals is thought to provide the feedback which regulates global climate over geological timescales (e.g. Walker et al., 1981; Berner et al., 1983). However quantifying the feedback and its response to the multiple controlling processes has proved difficult and controversial (e.g. Berner et al., 1983; Sundquist, 1991; Raymo, 1994). The difficulties arise from two sources. At a global scale, the total chemical weathering flux is dominated by carbonate and estimates of the smaller silicate weathering flux are subject to large uncertainties. Secondly the mechanisms which moderate the silicate weathering flux are poorly understood leading to large uncertainties in models of the climatic response to changes in forcing.

The climatic response of chemical weathering is usually considered a function of temperature and runoff (e.g. Berner et al., 1983; Velbel, 1993; White and Blum, 1995; White et al., 1998; Dessert et al., 2001). However, the climatic forcing has remained elusive in active orogens because of the strong lithological dependence of chemical weathering (Bluth and Kump, 1994; Gaillardet et al., 1999), and the close juxtaposition of different lithological domains. Recent studies of riverine chemistry in active orogens have been able to identify a climatic sensitivity of silicate weathering, by carefully selecting small catchments or by considering soil profiles (e.g. Riebe et al., 2001; France-Lanord et al., 2003; Jacobson et al., 2003; West et al., 2005). However, the relative importance of runoff and temperature remains controversial (Riebe et al., 2001) with many studies focussing on short term climatic forcing. The debate is central to the question as to whether exhumation of major orogens cools global climate by enhancing the silicate-weathering feedback.

This study considers data from Himalayan catchments, draining dominantly uniform lithologies. Constraining

* Corresponding author. Fax: +44 1223 333450.
E-mail address: ett20@esc.cam.ac.uk (E.T. Tipper).

climatic variations in weathering fluxes from the Himalaya is of particular importance because of the factor of 12 seasonal variation in runoff (Sharma, 1997) and because of the global impact of large Himalayan rivers on seawater (Richter et al., 1992). We show that outputs from Himalayan catchments exhibit seasonal variations in the relative magnitudes of the silicate and carbonate weathering fluxes which suggest a climatic sensitivity of the weathering processes and ultimately may be controlled by the local hydrology.

Seasonal variations in major elements, radiogenic isotopes and stable isotopes have already been reported in the Himalaya over large spatial scales (Sarin et al., 1989; Galy and France-Lanord, 1999; Hasnain and Thayyen, 1999; Krishnaswami et al., 1999; Bhatt et al., 2000; Karim and Veizer, 2000; Dalai et al., 2002a,b, 2003; Bickle et al., 2003; France-Lanord et al., 2003; Oliver et al., 2003; Quade et al., 2003; Evans et al., 2004; Singh et al., 2005). However, the interpretation of large scale variations is frustrated by the diverse lithologies across catchments, making it difficult to distinguish whether there is a fundamental change in the response of carbonate and silicate mineral weathering in situ in a catchment between the seasons, or whether inter-seasonal variability is a response to rainfall sampling distinct lithologies at different times of the year. Published results obtained so far, at medium geographic scales (either by time-series sampling or spot sampling between the wet and dry season) indicate a greater input of carbonate de-

rived ions in the monsoon (e.g. Galy and France-Lanord, 1999; Krishnaswami et al., 1999; Bickle et al., 2003; Quade et al., 2003). Krishnaswami et al. (1999) propose that this is because of the dominance of physical erosion during the wet season allowing more easily weatherable carbonates to dissolve. Bickle et al. (2003) attribute seasonal variations to result from variable inputs from the different Himalayan lithotectonic units because of spatially variable rainfall and glacial melt. Galy and France-Lanord (1999) suggested that the dissolution of soil carbonate may contribute to the chemical signal in their study.

In the present study, sample sites have been selected from the Marsyandi river (Nepal Himalaya) to sample only one major geological unit. Four new weekly time-series of river water samples spanning the 2002 and 2003 monsoon season are complemented by data from small tributaries comparing the wet and dry seasons. The data shows that even in first order catchments of several km², there is a systematic and significant change in both ⁸⁷Sr/⁸⁶Sr and major elements between the wet and dry season. Bedrock and bedload compositions have been analysed to constrain the lithological control on river chemistry.

The advantage of studying small catchments is that changes in the location of precipitation, resulting in runoff sampling distinct lithology, can be precluded as a control on water chemistry. Any seasonal variations in river chemistry must relate to a change in weathering process driven by the change in climate between the wet and dry season,

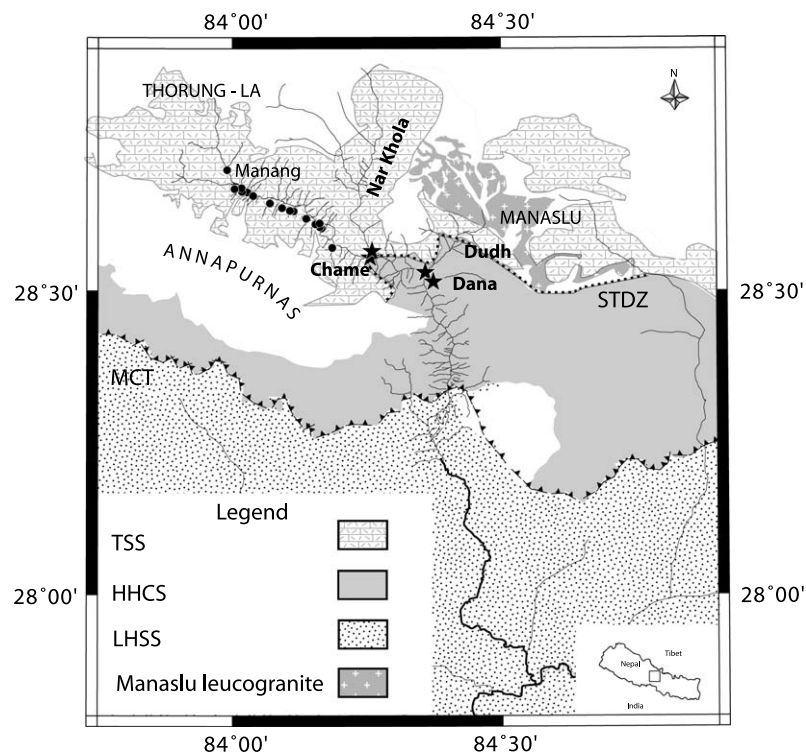


Fig. 1. Map of Marsyandi after Colchen et al. (1986). Time-series sampling sites are shown by the 4 large black stars. Tributaries sampled in both April and September are indicated by black circles. The main range strikes East–West between the Annapurnas and Manaslu. STDZ is the South Tibetan Detachment Zone and MCT is the Main Central Thrust. White areas are either glaciated or unmapped.

which is extreme in these Himalayan rivers. We interpret that to a first order the seasonal variations are caused by different proportions of carbonate and silicate weathering with a greater carbonate input in the monsoon.

The new data raise a series of questions about the mechanisms controlling carbonate and silicate weathering. In particular our results suggest that carbonate weathering has a greater sensitivity to runoff because of the faster dissolution kinetics of carbonate relative to silicate. We speculate that silicate weathering may be more important in waters with a longer residence time such as ground water. The large magnitude of the seasonal variations may have implications for the response of global silicate weathering fluxes to changes in the intensity of the monsoon recorded in the Bengal fan (e.g. France-Lanord et al., 1993), the interpretation of chemical proxies of recent climate change preserved in lake sediments (e.g. Holmes, 1996) and models for changes in chemical weathering rates with glacial–interglacial cycles (Gibbs and Kump, 1994).

2. Study area

The Marsyandi drains the Annapurna Himalaya, Nepal. The headwaters of the Marsyandi are in the Tethyan Sedimentary Series (TSS) with arid and glacial conditions, at an altitude of mostly >3500 m (Fig. 1). In the rain shadow of the main range, monsoonal rainfall is less than 0.5 m (Burbank et al., 2003). Glacial meltwater contributes significantly to the flux of water in certain tributaries. The Marsyandi drains a 50 km transect of the TSS. The bedrock is comprised of a continental margin sequence of variably metamorphosed impure limestone and siliclastic rocks including pyrite rich black shale interbedded at all scales. No evaporites have been reported (Bordet et al., 1971). There is a progressive increase in metamorphic grade from North to South, with Jurassic fossiliferous argillaceous limestone interbedded with occasional sandstone in the North. In the lower TSS a unit of amphibole calc-silicates with biotite, muscovite and chlorite outcrops above the South Tibetan Detachment Zone (Coleman, 1996; Searle and Godin, 2002). Vegetation is sparse in the TSS. The chemistry of TSS rivers has been described previously and is characterized by high total dissolved solids (Galy and France-Lanord, 1999; Bickle et al., 2005). Two of the time series sampling sites in the present study drain only the TSS: the upper Marsyandi and the Nar.

South of the TSS the Marsyandi incises the High Himalayan Crystalline Series (HHCS) which underlies the high mountains and consists of two main units. Formation 1 is dominated by silicate gneiss (Bordet et al., 1971; Le Fort, 1975) and Formation 2 is dominated by calc-silicate metamorphic rocks. The calc-silicate mineralogy comprises widespread diopside, amphibole, quartz, plagioclase and calcite assemblages with rarer pure calcite and diopside marbles (Bordet et al., 1971). Two tributaries (Dudh and Dana Khola) draining Formation 2 have been sampled in this study, though the head waters of the Dudh Khola also

Table 1
Major cations and anions and Sr isotope data for small TSS tributaries sampled in September 2002 (late monsoon)

Sample (September)	Sample (April)	Date	N (°)	E (°)	T	pH	Ca (μmol/l)	K (μmol/l)	Mg (μmol/l)	Na (μmol/l)	Si(OH) ₄ (μmol/l)	Sr (μmol/l)	Cl (μmol/l)	SO ₄ (μmol/l)	HCO ₃ (μmol/l)	⁸⁷ Sr/ ⁸⁶ Sr	TDS (mg/l)	SI _{cc}
ett12	ct29	06-Sep	28.610	84.150	9.3	8.7	667	59	174	21	22	0.75	10	168	1408	0.72431	137	0.46
ett14	ct14	07-Sep	28.620	84.140	13.4	8.3	1284	20	618	120	129	2.96	15	439	3040	0.73103	301	0.75
ett16	ct15	07-Sep	28.630	84.110	10.4	8.5	1177	19	203	32	52	1.37	17	193	2402	0.73057	222	0.78
ett17	ct16	07-Sep	28.630	84.110	11.8	8.6	1687	8	766	20	46	1.84	9	1299	2324	0.71936	356	0.92
ett18	ct17	07-Sep	28.640	84.090	12.4	8.6	1336	21	765	30	43	2.40	8	846	2550	0.71881	313	0.92
ett20	ct18	07-Sep	28.650	84.070	11.4	8.5	838	23	516	37	33	2.21	12	465	1820	0.71702	206	0.50
ett22	ct20	07-Sep	28.660	84.020	8.7	8.5	1147	30	608	132	39	3.55	17	942	1766	0.71757	265	0.51
ett23	ct19	08-Sep	28.660	84.030	8.7	8.3	1396	18	732	294	68	0.06	8	1180	2189	0.71722	330	0.49
ett24	ct27	08-Sep	28.660	84.040	16.0	8.1	1408	17	1577	201	135	5.51	16	967	4233	0.72256	455	0.70
ett28	ct32	08-Sep	28.660	84.020	6.0	8.4	723	20	275	18	22	1.62	4	412	1203	0.72477	151	0.12
ett29	ct21	08-Sep	28.670	84.020	11.7	8.6	1573	18	683	146	57	4.94	7	1245	2171	0.71824	338	0.88
ett30	ct31	09-Sep	28.670	84.000	6.8	8.5	933	31	589	93	43	2.62	6	664	1832	0.72266	232	0.51
ett34	ct23	10-Sep	28.700	83.990	7.2	8.7	1500	21	660	305	49	6.06	10	1141	2348	0.71478	339	0.91
ett61	ct33	14-Sep	28.610	84.160	11.4	8.6	761	13	810	21	47	2.13	7	602	1954	0.71295	230	0.51
ett63	ct36	14-Sep	28.571	84.186	na	na	721	24	121	16	27	1.21	28	10	1723	0.71438	142	na

The April sample numbers are from Bickle et al. (2005). SI_{cc} is the calcite saturation index calculated using PHREEQC.

Table 2
Major cations and anions and Sr isotope data for TSS rivers, sampled repeatedly in 2002 and 2003

Sample	Date	Ca ($\mu\text{mol/l}$)	K ($\mu\text{mol/l}$)	Mg ($\mu\text{mol/l}$)	Na ($\mu\text{mol/l}$)	Si(OH) ₄ ($\mu\text{mol/l}$)	Sr ($\mu\text{mol/l}$)	Cl ($\mu\text{mol/l}$)	SO ₄ ($\mu\text{mol/l}$)	HCO ₃ ($\mu\text{mol/l}$)	⁸⁷ Sr/ ⁸⁶ Sr	TDS (mg/l)
<i>Marsyandi at Chame (2002)</i>												
CT10	25-Apr	914	29	481	113	44	2.43	25	492	1914	0.71930	219
MT65	13-Jun	721	24	256	45	25	1.51	na	284	na	0.71764	na
MT66	19-Jun	718	23	249	40	24	1.49	na	275	na	0.71741	na
MT67	25-Jun	737	23	233	49	25	1.51	na	273	na	0.71681	na
MT17	26-Jul	782	32	280	88	27	1.78	28	378	1460	0.71700	169
MT18	01-Aug	832	31	307	110	28	2.08	34	455	1476	0.71623	181
MT19	07-Aug	836	28	337	91	32	2.08	34	459	1517	0.71724	184
MT20	14-Aug	890	29	355	97	30	2.35	25	551	1493	0.71633	194
MT21	21-Aug	883	28	349	117	29	2.24	31	560	1462	0.71656	193
MT22	28-Aug	960	29	445	110	39	2.65	29	646	1633	0.71721	217
MT23	03-Sep	973	28	473	123	39	2.86	31	714	1591	0.71688	222
MT24	09-Sep	972	31	475	150	45	2.63	47	637	1757	0.71811	227
ett69	14-Sep	947	29	458	104	46	2.67	36	647	1604	0.71860	215
MT25	16-Sep	988	31	488	154	47	2.67	148	640	1714	0.71832	229
MT26	23-Sep	1014	30	539	131	53	2.82	39	663	1910	0.71852	241
MT27	29-Sep	987	33	518	138	56	2.70	46	612	1917	0.71877	236
MT28	05-Oct	1010	31	548	144	57	2.90	46	654	1944	0.71863	243
MT29	12-Oct	1037	33	602	158	61	3.08	51	719	1989	0.71868	255
MT30	19-Oct	1038	34	613	170	64	3.13	60	730	1995	0.71879	257
MT31	26-Oct	1048	35	627	211	64	3.20	75	750	2022	0.71868	263
MT32	31-Oct	1025	36	618	212	65	3.12	82	709	2039	0.71902	259
MT107	30-Dec	901	46	608	244	68	3.13	113	710	1782	0.71945	241
<i>Marsyandi at Chame (2003)</i>												
MT108	17-Mar	921	43	675	178	59	3.41	63	779	1807	0.71911	248
MT109	19-Mar	902	49	614	239	66	3.20	130	10	3209	0.71952	263
MT110	17-Apr	823	35	506	151	51	2.63	85	598	1561	0.71971	207
MT111	25-Apr	753	33	422	107	35	2.23	49	497	1448	0.71927	183
MT112	26-Apr	735	32	395	120	37	2.09	70	455	1430	0.71949	178
MT155	07-Jul	805	30	334	107	32	2.11	42	421	1532	0.71710	181
MT156	14-Jul	747	26	281	80	30	1.78	26	355	1427	0.71738	163
MT157	21-Jul	857	28	377	112	33	2.51	34	417	1744	0.71579	196
MT158	28-Jul	751	28	287	96	30	1.80	32	350	1468	0.71793	166
MT159	09-Aug	788	31	348	104	35	2.13	34	10	2418	0.71780	196
MT160	15-Aug	794	32	321	100	33	1.97	36	407	1513	0.71762	177
MT161	24-Aug	799	30	364	116	37	2.16	36	476	1487	0.71801	184
<i>Nar (2002)</i>												
CT9	25-Apr	1317	29	793	184	61	3.94	26	1053	2288	0.71520	321
MT62	13-Jun	na	48	604	130	na	4.22	na	588	na	na	na
MT63	19-Jun	867	28	394	100	29	2.84	na	600	na	0.71402	na
MT64	25-Jun	887	30	345	118	28	3.32	na	554	na	0.71284	na
MT1	26-Jul	973	31	429	143	29	3.22	22	791	1378	0.71378	216
MT2	01-Aug	897	27	337	102	25	2.49	16	579	1426	0.71425	192
MT3	07-Aug	1034	25	466	122	30	3.31	15	847	1448	0.71405	228
MT4	14-Aug	1064	26	513	125	30	3.54	22	960	1370	0.71394	237
MT5	21-Aug	1128	29	545	166	31	3.74	28	1031	1457	0.71383	253
MT6	28-Aug	1271	29	705	167	37	4.63	16	1262	1622	0.71444	295
MT7	03-Sep	1278	29	731	177	38	4.88	67	1338	1493	0.71452	297
MT8	09-Sep	1311	30	784	212	46	4.59	30	1307	1798	0.71379	315
ett74	15-Sep	1436	28	834	163	49	5.19	28	1042	1973	0.71443	207
MT9	16-Sep	1282	27	777	195	47	4.45	27	1272	1782	0.71444	309
MT10	23-Sep	1422	30	903	191	59	4.94	14	1426	2022	0.71474	347
MT11	29-Sep	1390	30	866	186	59	4.70	18	1347	2033	0.71470	338
MT12	05-Oct	1321	29	812	177	57	4.46	20	1290	1887	0.71478	319
MT13	12-Oct	1445	31	948	200	67	5.12	42	1469	2057	0.71479	356
MT14	19-Oct	1430	32	959	202	69	5.00	21	1429	2152	0.71491	357
MT15	26-Oct	1403	31	944	240	69	4.94	34	1487	1972	0.71498	352
MT16	31-Oct	1435	33	975	245	71	5.00	40	1444	2187	0.71506	363
MT113	24-Dec	1211	34	916	209	77	4.96	36	1316	1843	0.71544	318
MT114	30-Dec	1334	40	935	211	110	5.05	84	1300	2119	0.71535	341

Table 2 (continued)

Sample	Date	Ca ($\mu\text{mol/l}$)	K ($\mu\text{mol/l}$)	Mg ($\mu\text{mol/l}$)	Na ($\mu\text{mol/l}$)	Si(OH) ₄ ($\mu\text{mol/l}$)	Sr ($\mu\text{mol/l}$)	Cl ($\mu\text{mol/l}$)	SO ₄ ($\mu\text{mol/l}$)	HCO ₃ ($\mu\text{mol/l}$)	⁸⁷ Sr/ ⁸⁶ Sr	TDS (mg/l)
<i>Nar (2003)</i>												
MT115	01-Apr	1210	34	927	205	79	4.83	35	1313	1870	0.71561	320
MT116	17-Apr	1120	34	854	206	69	4.52	34	1216	1738	0.71552	297
MT162	07-Jul	851	24	388	104	31	2.74	5	631	1344	0.71431	191
MT163	14-Jul	892	25	406	119	32	2.77	47	653	1389	0.71443	200
MT164	21-Jul	947	26	464	130	32	3.31	8	762	1452	0.71384	216
MT165	28-Jul	876	24	416	120	31	2.96	9	683	1357	0.71402	199
MT166	09-Aug	1000	28	555	143	36	3.85	3	895	1495	0.71386	236
MT167	15-Aug	931	25	454	110	32	2.98	7	742	1423	0.71433	211
MT168	24-Aug	1117	29	643	168	40	4.11	32	1029	1640	0.71412	267

drain the Manalsu leucogranite and some TSS exposures. Monsoonal rainfall is at its maximum in these catchments (up to 4 m (Burbank et al., 2003)) and there is significant vegetation with forested valley sides. The chemistry of HHCS rivers is characterized by low total dissolved solids. HHCS rivers receive input from hydrothermal systems in the Marsyandi (Evans et al., 2001, 2004), and the rivers analysed in this study have been corrected for this input.

3. Data collection and analysis

Tables 1–3 list the chemical and isotopic analyses of 140 water samples collected from the four Marsyandi catchments. Samples were collected on a weekly or monthly basis during 2002 and 2003, including the monsoon (Tables 2 and 3). Small tributaries from the TSS were collected in April 2002 (premonsoon) and their chemical data are published in Bickle et al. (2005). The same tributaries were sampled in September (monsoon) and are compared to those of Bickle et al. (2005) in this study (Table 1). Water samples were filtered on collection through 0.1 μm cellulose nitrate filters. A 30 ml fraction for cation analysis was collected into a polyethylene bottle, pre-acidified with quartz distilled HCl. A further 15 ml fraction was collected for anion analysis without acidification. Water samples were analysed for cations (Ca, K, Mg, Na, S, Si, and Sr) by ICP-AES in Cambridge against synthetic standards. Repeat analysis of natural water standards ION 20 and SPSSW2 demonstrates a reproducibility within 3% (2 standard deviations $n = 84$ and 72 , respectively), over the two year period of analyses of the Marsyandi waters. Analysed concentrations were within 3% of published values. Cl, SO₄, and NO₃ were analysed at the Institut de Physique du Globe, Paris, the University of Keele and the Open University by ion chromatography. Molar SO₄ and S analysed by ion chromatography and AES agree to within 0.27% ($2\sigma_m$). HCO₃ was determined by gran titration for the April tributary collections and by charge balance for the other samples. These methods have been shown to be reliable to within 10% in Himalayan rivers where organic acids are dilute (Galy and France-Lanord, 1999). Temperature and pH were measured at the sampling site in April and September. A representative collection of rock and bedload

have been analysed for major elements at the Open University by XRF following Ramsey et al. (1995). ⁸⁷Sr/⁸⁶Sr isotope analyses were performed on a T40 Sector 54 VG mass spectrometer at Cambridge following Bickle et al. (2003). Analyses of NBS987 prior to May 2003 averaged 0.710235 ± 0.000011 and analyses after this averaged 0.710253 ± 0.000008 . Total procedural blanks over the period of analyses yielded 131 pg/g of Sr, negligible compared to the amount of Sr processed.

4. Cyclic and hydrothermal corrections

Input from rain or dry deposition can be significant to river waters. All rivers have been corrected for cyclic input based on the rain data of Galy and France-Lanord (1999) (Table 4) following the correction method of Bickle et al. (2003). There is a significant hydrothermal input to the rivers of the Marsyandi (Evans et al., 2001, 2004; Becker, 2005) with numerous hot springs close to the Main Central Thrust. The rivers in this study are all north of the Main Central Thrust (Fig. 1) and there is a relatively limited hydrothermal input, as evidenced by the low Cl concentrations (mean 40 μmol) compared to the Marsyandi immediately after the main hot spring input further downstream at 700 μmol (Evans et al., 2001). Rivers have been corrected for Cl in excess of rain following the method of Bickle et al. (2003) and using a compilation of hot spring data from Evans et al. (2001) and Becker (2005) (Table 4). ⁸⁷Sr/⁸⁶Sr has been corrected in a similar manner for both rain and hydrothermal input. For TSS rivers, the correction results in a mean 4% difference in total dissolved solids (TDS), a 2% difference in dissolved Sr and a 0.000230 difference in ⁸⁷Sr/⁸⁶Sr. For HHCS, rivers there is a mean 10% difference in TDS, a 13% difference in dissolved Sr and 0.000560 difference in ⁸⁷Sr/⁸⁶Sr. Figures are presented with both corrected and uncorrected data.

5. Seasonal variations

Mainstem major element chemistry and Sr isotope ratios show significant seasonal variations. Concentrations of the major cations decrease by a factor of 2–4 during the monsoon compared to the dry winter months (Fig. 2), with the

Table 3
Major cations and anions and Sr isotope data for HHCS rivers, sampled repeatedly in 2002 and 2003

Sample	Date	Ca ($\mu\text{mol/l}$)	K ($\mu\text{mol/l}$)	Mg ($\mu\text{mol/l}$)	Na ($\mu\text{mol/l}$)	Si(OH) ₄ ($\mu\text{mol/l}$)	Sr ($\mu\text{mol/l}$)	Cl ($\mu\text{mol/l}$)	SO ₄ ($\mu\text{mol/l}$)	HCO ₃ ($\mu\text{mol/l}$)	⁸⁷ Sr/ ⁸⁶ Sr ($\mu\text{mol/l}$)	TDS (mg/l)
<i>Dudh (2002)</i>												
CT7	24-Apr	483	27	39	117	89	0.47	53	67	974	0.72822	93
MT72	01-Jun	456	18	34	64	54	0.38	na	52	na	0.72550	na
MT73	18-Jun	430	18	33	49	68	0.36	na	50	na	0.78662	na
MT74	26-Jun	450	17	32	43	51	0.36	na	50	na	0.72602	na
MT47	26-Jul	460	15	35	44	50	0.38	18	73	844	0.72534	81
MT48	02-Aug	464	14	36	44	48	0.40	17	63	873	0.72330	82
MT49	09-Aug	466	13	33	35	46	0.38	18	65	902	0.72467	84
MT50	16-Aug	440	13	33	37	46	0.37	17	66	850	0.72515	79
MT51	23-Aug	413	12	31	44	49	0.34	15	58	772	0.72508	73
MT52	30-Aug	444	15	37	52	63	0.39	37	73	848	0.72636	81
MT53	06-Sep	444	14	36	47	62	0.39	50	64	845	0.72467	80
MT54	13-Sep	427	14	35	51	72	0.38	24	59	850	0.72625	79
ett96	17-Sep	435	14	36	60	78	0.39	38	64	842	0.72632	80
MT55	20-Sep	478	16	40	70	88	0.43	36	64	961	0.72618	89
MT56	27-Sep	444	15	36	60	82	0.40	30	55	897	0.72649	82
MT57	04-Oct	472	17	39	73	89	0.43	35	59	959	0.72728	88
MT58	11-Oct	506	17	43	87	101	0.47	44	63	1034	0.72699	96
MT59	18-Oct	507	18	44	95	101	0.48	48	65	1038	0.72671	97
MT60	25-Oct	503	18	43	94	99	0.47	49	62	1033	0.72713	96
MT97	22-Dec	516	21	46	126	111	0.49	71	60	1152	0.72733	105
MT98	28-Dec	527	22	46	142	118	0.51	114	59	1191	0.72677	110
<i>Dudh (2003)</i>												
MT99	02-Jan	543	21	49	139	119	0.53	117	89	1221	0.72664	115
MT100	14-Apr	494	57	50	152	323	0.44	81	65	1187	0.72830	109
MT101	01-May	542	21	48	141	119	0.53	85	64	1222	0.72653	112
MT142	29-Jul	492	21	53	94	61	0.57	67	67	1024	0.72217	96
MT143	05-Aug	528	24	37	88	58	0.49	229	54	1097	0.72387	106
MT144	20-Aug	421	20	35	83	57	0.42	70	47	895	0.72453	83
MT145	23-Aug	487	20	58	87	56	0.57	35	75	1007	0.72212	95
MT146	27-Aug	459	18	34	71	58	0.44	33	57	940	0.72480	86
<i>Dana (2002)</i>												
CT41	04-May	540	24	31	52	75	0.46	31	97	980	0.72130	96
MT68	11-Jun	462	22	30	25	52	0.38	na	93	na	0.72196	na
MT69	18-Jun	466	22	30	27	54	0.38	na	96	na	0.72160	na
MT70	26-Jun	452	21	28	29	47	0.37	na	91	na	0.72162	na
MT33	26-Jul	426	18	26	20	51	0.34	9	73	787	0.72112	75
MT34	02-Aug	422	18	28	27	43	0.35	11	71	794	0.72008	75
MT35	09-Aug	436	18	31	28	42	0.39	14	77	813	0.71983	78
MT36	16-Aug	435	20	31	55	45	0.38	27	87	809	0.72013	80
MT37	23-Aug	431	18	25	21	49	0.33	14	69	800	0.72082	76
MT38	30-Aug	491	21	36	36	57	0.44	43	93	885	0.71992	87
MT39	06-Sep	448	20	33	55	56	0.40	25	79	856	0.71995	82
MT40	13-Sep	489	22	31	39	64	0.41	17	75	937	0.72022	88
ett95	17-Sep	491	19	27	30	66	0.56	11	78	909	0.72072	86
MT41	20-Sep	519	22	30	37	70	0.42	22	77	984	0.72040	92
MT42	27-Sep	482	21	28	57	68	0.39	28	74	923	0.72035	87
MT43	04-Oct	520	21	30	32	70	0.41	11	82	980	0.72079	92
MT44	11-Oct	544	22	30	37	77	0.43	18	81	1030	0.72078	96
MT45	18-Oct	538	22	29	40	75	0.42	18	83	1015	0.72078	96
MT46	25-Oct	549	31	30	60	75	0.43	46	91	1024	0.72077	99
MT102	22-Dec	531	25	33	50	92	0.42	24	82	1011	0.72114	96
<i>Dana (2003)</i>												
MT104	02-Jan	536	24	31	50	82	0.42	43	92	969	0.72107	95
MT105	14-Apr	534	24	33	51	77	0.43	23	88	1006	0.72109	96
MT106	01-May	537	23	32	51	85	0.42	26	89	1000	0.72130	96
MT151	06-Aug	430	20	26	37	49	0.39	25	63	816	0.72002	77
MT152	20-Aug	413	22	33	62	56	0.41	25	56	833	0.72068	78
MT153	13-Aug	438	24	29	64	53	0.41	29	65	856	0.71967	81
MT154	27-Aug	444	20	27	38	54	0.40	13	58	867	0.72040	80

Table 4

Cation to Cl molar ratios and errors of rain (Galy and France-Lanord, 1999; Bickle et al., 2003) and hot springs (Becker, 2005) used to make cyclic and hydrothermal corrections to the data set ($^{\text{a}}\text{nmol}/\mu\text{mol}$)

	Ca/Cl	Mg/Cl	K/Cl	Na/Cl	Si/Cl	Sr/Cl ^a	⁸⁷ Sr/ ⁸⁶ Sr
Rainfall	2.97	1.99	0.72	1.35	0.41	4.05	0.7137
2 σ	0.42	0.28	0.10	0.19	0.06	0.57	0.0006
Hot spring	0.16	0.03	0.10	0.41	0.01	1030	0.739
2 σ	0.05	0.01	0.03	0.12	0.004	308	—

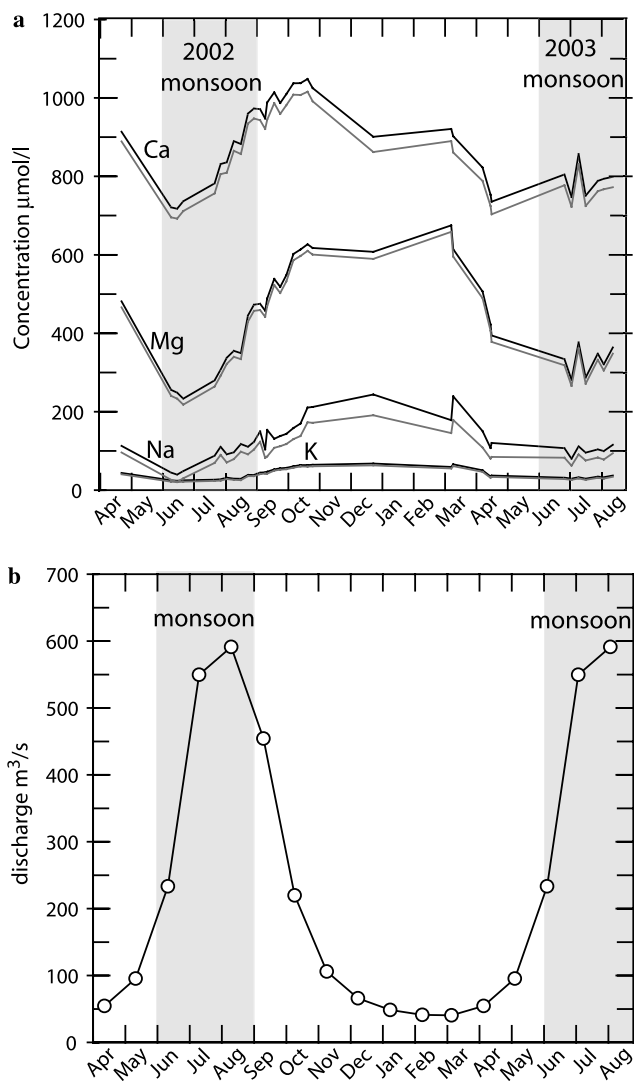


Fig. 2. (a) Cation concentrations throughout the annual hydrological cycle, from the Marsyandi at Chame. The black lines are uncorrected data and the grey lines are corrected for cyclic and hydrothermal input. (b) Monthly discharge in the Marsyandi averaged over 10 year period from the Lesser Himalaya near the confluence with the Trisuli (Sharma, 1997).

exception of Ca which only decreases by a factor of 1.5. Discharge increases by a factor of up to 12 (Sharma, 1997; Gabet et al., 2004). The variation in concentration relates to monsoonal dilution (Galy and France-Lanord, 1999). Concentrations in the 2002 monsoon are lower than in 2003 consistent with reports that the 2002 monsoon was of exceptional magnitude (Bookhagen et al., 2005). Varia-

tions in ⁸⁷Sr/⁸⁶Sr must relate to changing the proportion of Sr derived from different minerals, rather than just monsoonal dilution. Changes in elemental ratios relate to either changing source or because of differential dissolution/precipitation rates between minerals, in particular carbonate and silicate minerals, between the wet and dry season. As a consequence, most of the data in this study is presented as elemental ratios as these prove insightful in tracing either source or weathering process. Time-series variations are considered first before comparing small tributaries between the wet and dry season.

5.1. Seasonal cation variations

In each of the four rivers where a time-series was collected there are systematic trends in cation ratios. All cation to Ca ratios decrease by a factor of ca. 2 in the monsoon compared to the dry season. As an example, the $\text{Si}(\text{OH})_4/\text{Ca}$ ratio is presented (Fig. 3). In the rivers draining TSS (Marsyandi and Nar) the $\text{Si}(\text{OH})_4/\text{Ca}$ ratios are closely matched ranging from 0.08 in the dry season to 0.02–0.03 in the monsoon. The rivers draining the HHCS have a higher $\text{Si}(\text{OH})_4/\text{Ca}$ at all times of the year than TSS rivers, consistent with previous data from the Himalaya and reflecting a lithological influence on river chemistry (e.g. Krishnaswami et al., 1999; English et al., 2000). The range in the HHCS rivers (Dudh and Dana) is 0.23 in the dry season to 0.09 in the monsoon. The Dana Khola exhibits a less well defined trend but the systematic decrease in the monsoon is apparent (Fig. 3). The post monsoon period of 2002 shows a very systematic increase in $\text{Si}(\text{OH})_4/\text{Ca}$ in all four rivers and the close correspondence in the detail of the curves suggests a single control on four spatially different rivers (Fig. 3). The Marsyandi at Chame shows a decrease in $\text{Si}(\text{OH})_4/\text{Ca}$ before the onset of the 2003 monsoon. It is not clear why this is the case but it may arise from local orographic precipitation patterns or spring melt water runoff.

5.2. Seasonal Sr isotope variations

Each of the four rivers collected for time-series shows a distinct range in Sr isotope ratios (Fig. 3). The least radiogenic is the Nar river ranging from 0.713 to 0.716. The Marsyandi is more radiogenic ranging from 0.716 to 0.720. The HHCS rivers are even more radiogenic; the

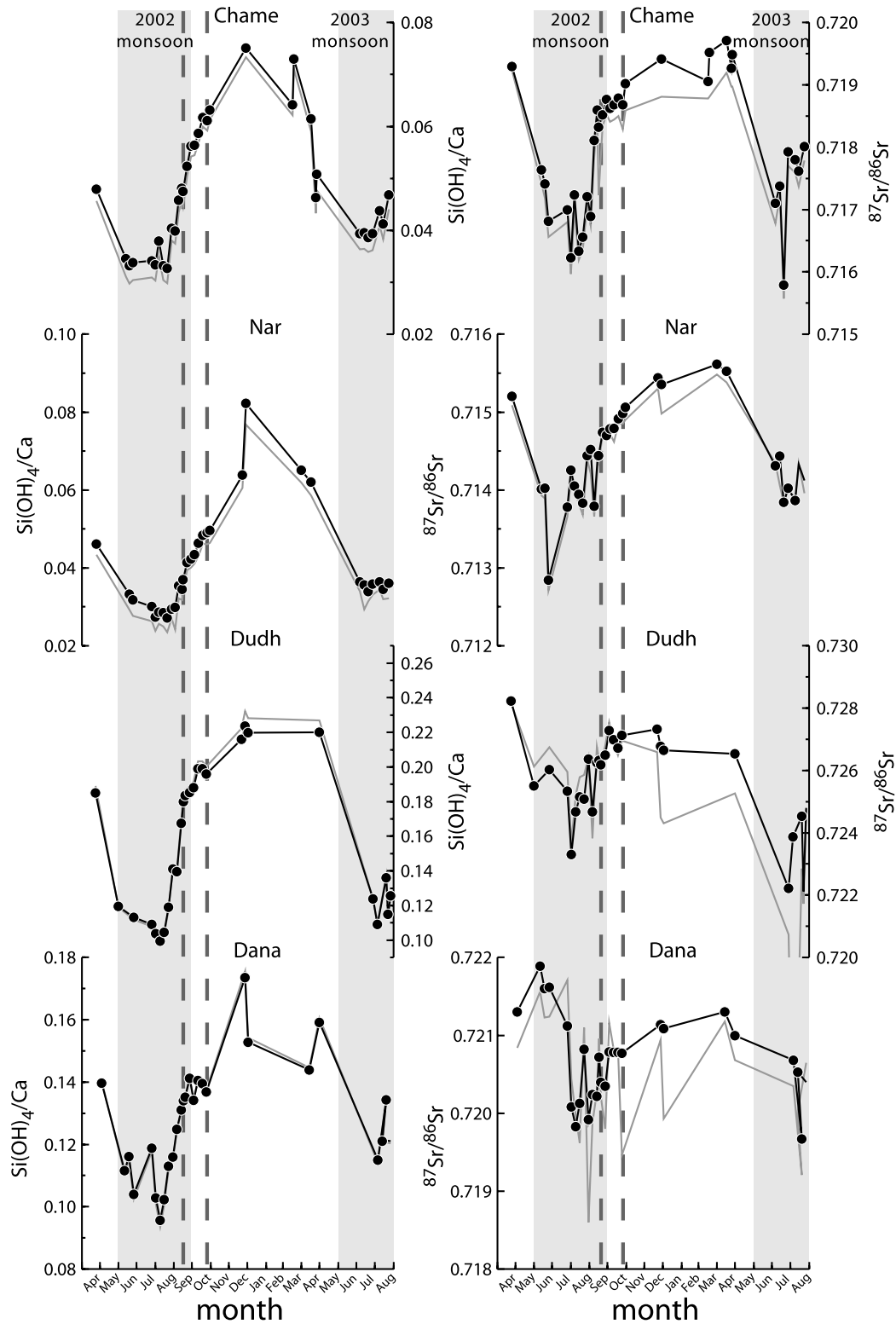


Fig. 3. Time-series data presented as $\text{Si(OH)}_4/\text{Ca}$ (left) and $^{87}\text{Sr}/^{86}\text{Sr}$ (right). Grey lines are corrected data. The vertical dashed line correlates small temporal variations between all four catchments, where the Marsyandi, Dudh and Dana all show a simultaneous minor decrease in $\text{Si(OH)}_4/\text{Ca}$.

Dana ranging from 0.719 to 0.722 and the Dudh ranging from 0.722 to 0.728. The Sr isotope results are consistent with $\text{Si(OH)}_4/\text{Ca}$ between the TSS and HHCS. TSS rivers have lower $\text{Si(OH)}_4/\text{Ca}$ and lower $^{87}\text{Sr}/^{86}\text{Sr}$ than HHCS rivers (Galy and France-Lanord, 1999; Jacobson et al.,

2002; Bickle et al., 2005). More subtle differences in the river chemistry, such as the higher $^{87}\text{Sr}/^{86}\text{Sr}$ in the Dudh than in the Dana, whilst these rivers have a similar signal in $\text{Si(OH)}_4/\text{Ca}$ almost certainly arise from local lithological variations. The Dudh samples some TSS lithologies and

the headwaters drain the Manalsu leucogranite. The Dana however only drains Formation 2. Despite small differences between the rivers, the seasonal trends are broadly similar.

There are systematic trends in all four rivers between the dry season and the monsoon season for Sr isotope ratios. In the early part of the 2002 and 2003 monsoon there is a rapid decrease in $^{87}\text{Sr}/^{86}\text{Sr}$ followed by a gradual increase post monsoon. The trends in TSS rivers are very clear with up to a 0.003 variation in $^{87}\text{Sr}/^{86}\text{Sr}$. The trends in HHCS rivers are less prominent compared to TSS rivers but systematically lower ratios in the monsoon are observed. The corrected ratios for cyclic and hydrothermal contribution show more scatter than uncorrected data because HHCS rivers are more sensitive to rain and hot spring inputs because they are more dilute.

5.3. Tributary variations

Fifteen tributaries from TSS catchments sampled by Bickle et al. (2005) in April (premonsoon) were re-sampled

for this study in September (monsoon). These catchments range in size from ca. 50 km² to only several km². The $\text{Si}(\text{OH})_4/\text{Ca}$, Na/Ca , K/Ca , and Sr isotope ratios have been compared between the premonsoon and monsoon water stage (Fig. 4). Most tributaries plot below the 1:1 line for $\text{Si}(\text{OH})_4/\text{Ca}$, Na/Ca , K/Ca and $^{87}\text{Sr}/^{86}\text{Sr}$, demonstrating that on average tributaries have lower ratios in the monsoon. This is consistent with the time-series data from the larger rivers (Sections 5.1 and 5.2). The combination of spot sampling of small tributaries and time-series sampling confirms that the trends observed by other studies occur at small spatial scales (e.g. Galy and France-Lanord, 1999) where only one main lithology is drained. Given that the catchments in the present study drain either TSS or HHCS the variations are not specific to a single rock type.

5.4. Seasonal variations from other Himalayan catchments

The seasonal variations presented for the Marsyandi are not unique in the Himalaya and are observed in two other

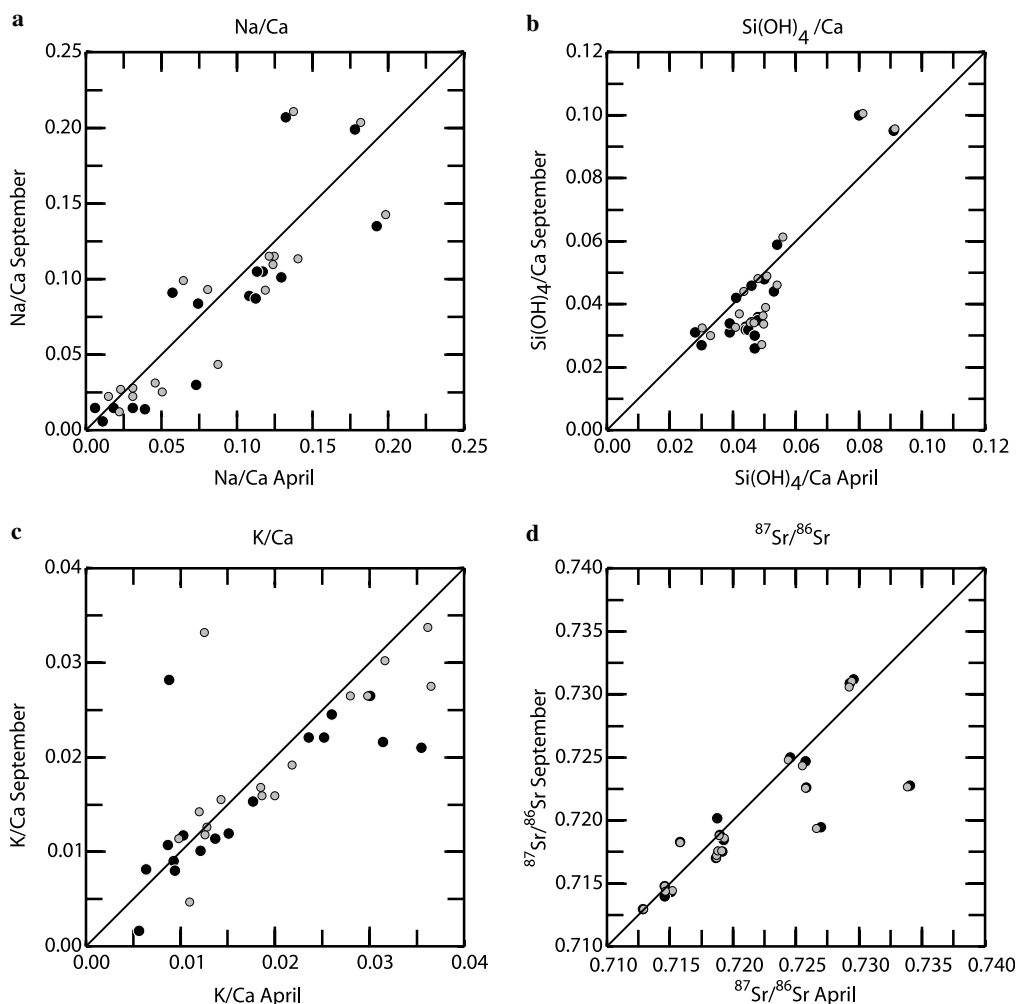


Fig. 4. Cross plots of tributary data from April (Bickle et al., 2005) and September (this study) for: (a) Na/Ca ratios, (b) Si/Ca ratios, (c) K/Ca ratios and (d) Sr isotope ratios. Grey points are data not corrected for cyclic and hydrothermal input and black points are corrected. There is a general trend of ratios normalised to Ca to be lower in September, with the majority of tributaries falling below the 1:1 line. Sr isotope ratios are also lower in September in accordance with the data from the main river.

small monolithological catchments from the Langtang (Nepal) and the Garhwal Himalaya (India) (Hasnain and Thayyen, 1999; Bhatt et al., 2000). These small catchments (14 and 23 km², respectively) drain dominantly silicate formations of the HHCS. Greater than 50% of both catchment areas are glaciated. Both discharge and solute chemistry from the Langtang are reported in Bhatt et al. (2000) sampled during 1996. The Dokriani is situated in the Garhwal Himalaya of Uttar Pradesh, India. Solute chemistry and discharge are reported in Hasnain and Thayyen (1999) sampled over the 1994 monsoon season. Water samples have been corrected for cyclic input following West et al. (2002) and show negligible hydrothermal input. Sr isotope data is not available for these samples.

In these catchments the proportion of silicate to total weathering has been quantified by estimating the propor-

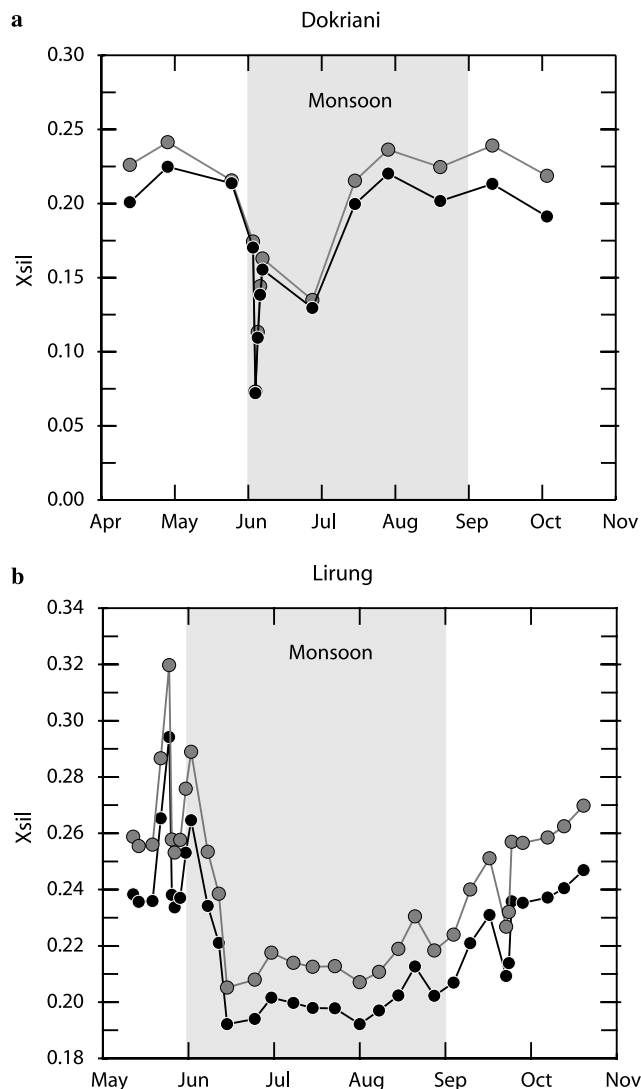


Fig. 5. X_{sil} seasonal variations for (a), the Dokriani and (b) the Langtang. Grey points are calculated using the rock ratios of Quade et al. (2003) and black points are calculated using the rock ratios of Gaillardet et al. (1999) and Galy and France-Lanord (1999). Although the magnitude of X_{sil} depends on the values of the rock cation ratios adopted, this choice should not alter their relative values.

tion of silicate to total ions leached during the weathering process following Krishnaswami et al. (1999) and Galy and France-Lanord (1999) and modified by Quade et al. (2003) (Fig. 6). Discharge data is available from these catchments and so it is useful to use this approach to quantify the carbonate and silicate weathering fluxes. Silicate Ca and Mg are calculated using the Ca/Na and Mg/Na ratio of silicate rocks where Ca_{sil} is calculated as

$$\text{Ca}_{\text{sil}} = \text{Na}^* \times \left(\frac{\text{Ca}}{\text{Na}} \right)_{\text{silicate rock}} \quad (1)$$

and Mg_{sil} is calculated as

$$\text{Mg}_{\text{sil}} = \text{Na}^* \times \left(\frac{\text{Mg}}{\text{Na}} \right)_{\text{silicate rock}} \quad (2)$$

Note that Na^* is Na corrected for cyclic and hot spring inputs. X_{sil} , the fraction of silicate cations to total cations is calculated on an equivalent basis as:

$$X_{\text{sil}} = \left(\frac{2 \times \text{Ca}_{\text{sil}} + 2 \times \text{Mg}_{\text{sil}} + \text{K} + \text{Na}}{2 \times \text{Ca} + 2 \times \text{Mg} + \text{K} + \text{Na}} \right) \quad (3)$$

The effect on X_{sil} of using different rock ratios has been assessed by using the Ca/Na_{sil} of Galy and France-Lanord (1999) at 0.2 and Quade et al. (2003) at 0.41. The same Mg/Na_{sil} as Quade et al. (2003) of 0.24 has been assumed to be typical of silicate rock ratios. Although there are large uncertainties in the appropriate silicate rock cation ratios the overall trends reported in this study do not depend on the values used unless incongruent silicate rock dissolution exhibits marked seasonal variation.

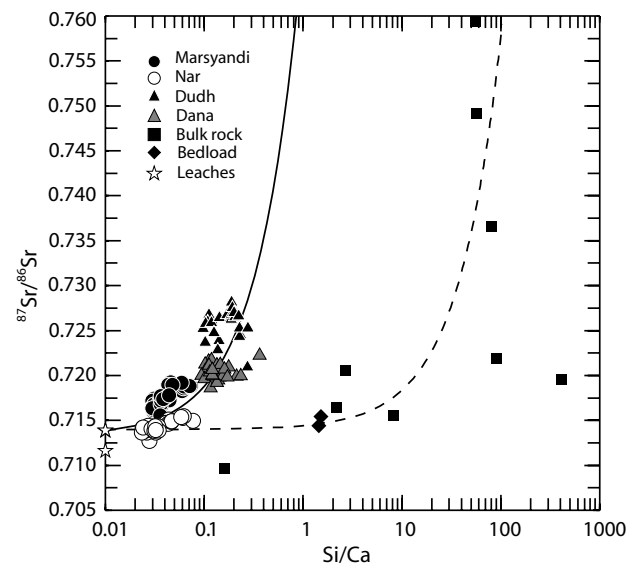


Fig. 6. Sr isotope and Si/Ca for bedrock, bedload and dissolved load. The dissolved load defines an array. The solid black line is the regression line through the all dissolved data ($R^2 = 0.59$). The dissolved load trends towards the Sr isotope values of the leachates as the carbonate end-member. Each catchment has slightly different characteristics reflecting the different proportion of carbonate and silicate bedrock in each catchment. The rock and bedload data also define an array. The dashed line is the regression line through the rock and bedload data ($R^2 = 0.79$).

This method assumes congruent dissolution of silicate rocks and conservative behaviour of solutes, assumptions that may be violated in certain cases. Incongruent dissolution is particularly likely in weathering limited areas with high erosion rates (Stallard, 1995). The most significant incongruent process affecting X_{sil} in these catchments is the removal of Ca by the precipitation of secondary carbonate which is common in Himalayan catchments (e.g. Galy et al., 1999; English et al., 2000; Jacobson et al., 2002; Bickle et al., 2005). This may cause an over estimation of X_{sil} .

X_{sil} is high in these silicate dominated catchments (Fig. 5), up to 35% in the Dokriani, consistent with rivers draining silicate bedrock. For comparison the average X_{sil} in the Dudh is 11%, 8% in the Dana and drops to as low as 3% in the Marsyandi at Chame and the Nar Khola during the monsoon. There are strong seasonal trends in both rivers. X_{sil} decreases by up to a factor of 2 during the monsoon. This is very similar to the trends in the $\text{Si}(\text{OH})_4/\text{Ca}$ and $^{87}\text{Sr}/^{86}\text{Sr}$ in the Marsyandi, demonstrating that the seasonal variations in weathering process are not restricted to catchments dominated by limestone or calc-silicate lithology. In these rivers, the variations cannot be related to changing hydrothermal input since the Lirung and Dokriani are catchments known to be free of springs.

6. Discussion

The seasonal variations in river chemistry have been presented as $\text{Si}(\text{OH})_4/\text{Ca}$, X_{sil} and $^{87}\text{Sr}/^{86}\text{Sr}$. These should all trace the proportion of silicate to carbonate derived ions. However, trends in $\text{Si}(\text{OH})_4/\text{Ca}$ and X_{sil} may be biased by the removal of Ca from river waters by secondary carbonate. $^{87}\text{Sr}/^{86}\text{Sr}$ is also known to be complicated in the Himalaya. The extent to which the seasonal variations represent changing the proportion of carbonate to silicate derived ions is first assessed, by considering the chemistry of the bedrock. The discussion then considers the controls on carbonate and silicate weathering, to explain the observed trends.

6.1. Carbonate to silicate control on Marsyandi waters

There are several different approaches of estimating the proportion of carbonate to silicate derived ions in river waters (e.g. Garrels and Mackenzie, 1967; Negrel et al., 1993; Gaillardet et al., 1999; Galy et al., 1999; Krishnaswami et al., 1999; Quade et al., 2003; Bickle et al., 2005). Ultimately these methods rely on combining rock ratios with river water cation data, in a similar way to X_{sil} of the present study (Section 5.4). In the Himalaya, it is accepted that Ca is not a conservative element (Galy et al., 1999; Jacobson et al., 2002; Bickle et al., 2005) because of the precipitation of secondary calcite. This can bias the calculation of the proportion of carbonate to silicate derived ions.

In the present study, the Marsyandi data has been presented as $\text{Si}(\text{OH})_4/\text{Ca}$ ratios and $^{87}\text{Sr}/^{86}\text{Sr}$ (Fig. 3). These can be used to qualitatively assess the proportion of silicate to carbonate derived ions in the solute load. $\text{Si}(\text{OH})_4/\text{Ca}$ is a qualitative tracer of silicate to carbonate in limestone dominated catchments where dissolved Ca is buffered by limestone dissolution. As noted above, however, all tracers of carbonate to silicate involving Ca are complicated because of the non-conservative behaviour of Ca. Up to 70% of the total dissolved Ca is reported to be removed from Himalayan rivers (Galy et al., 1999; Jacobson et al., 2002; Bickle et al., 2005) and soil carbonate has been observed in the Marsyandi catchment. $^{87}\text{Sr}/^{86}\text{Sr}$ is not affected by the precipitation of secondary calcite (Stewart et al., 1998) as any naturally occurring fractionations are normalised during analysis. In addition, the dissolution of secondary calcite will greatly affect the $\text{Si}(\text{OH})_4/\text{Ca}$ ratios while the $^{87}\text{Sr}/^{86}\text{Sr}$ will be barely modified since secondary calcite has a low Sr concentration (Tesoriero and Pankow, 1996). Given that the seasonal trends in $^{87}\text{Sr}/^{86}\text{Sr}$ and $\text{Si}(\text{OH})_4/\text{Ca}$ are similar (Fig. 3), the non conservative behaviour of calcite cannot alone account for the variations in $\text{Si}(\text{OH})_4/\text{Ca}$.

Because of the close correspondence and systematic variation of $\text{Si}(\text{OH})_4/\text{Ca}$ and $^{87}\text{Sr}/^{86}\text{Sr}$, we suggest that variability in both $^{87}\text{Sr}/^{86}\text{Sr}$ ratios and in major ion chemistry is dominated by variations in the relative inputs from carbonate and silicate sources. There is a continuing controversy as to the extent to which Sr isotope ratios in Himalayan rivers reflect a silicate Sr flux or a carbonate Sr flux with high $^{87}\text{Sr}/^{86}\text{Sr}$ ratios (e.g. Edmond, 1992; Krishnaswami et al., 1992; Palmer and Edmond, 1992; Pande et al., 1994; Quade et al., 1997; Harris et al., 1998; Galy et al., 1999; English et al., 2000; Bickle et al., 2003, 2005; Oliver et al., 2003). Where carbonate is highly radiogenic, particularly in the Lesser Himalaya (Singh et al., 1998; Galy et al., 1999; Bickle et al., 2001), it may be difficult to distinguish between carbonate and silicate Sr (Blum et al., 1998; Jacobson and Blum, 2000). However, none of the catchments in this study are from the Lesser Himalaya and carbonates from the Marsyandi HHCS and TSS are only moderately radiogenic, with leachates on bedload yielding $^{87}\text{Sr}/^{86}\text{Sr}$ of 0.712–0.714 (Galy et al., 1999) and the present study (Table 5).

Analysis of bedrock, bedload and dilute acid leaches of bedload from the Marsyandi demonstrates that carbonate and silicate $^{87}\text{Sr}/^{86}\text{Sr}$ are distinct in the Marsyandi (Table 5). The analyses define an array in $^{87}\text{Sr}/^{86}\text{Sr}$ – Si/Ca space with the bedload leaches defining a low $^{87}\text{Sr}/^{86}\text{Sr}$ and zero Si/Ca carbonate end-member (Fig. 6). Even at the confluence of the Marsyandi with the Trisuli in the Lesser Himalaya bedload leaches have $^{87}\text{Sr}/^{86}\text{Sr}$ ca. 0.713 similar to the leachate composition of TSS bedload and much lower than bulk bedload (0.736) which requires that the highly radiogenic carbonates of the Lesser Himalaya and HHCS only contribute a small fraction of the dissolved Sr in the Marsyandi.

Table 5
Bedrock, bedload, and leachate data from the Marsyandi catchment

Sample	Lithology	Type	N	E	wt% oxides								LOI	Total	⁸⁷ Sr/ ⁸⁶ Sr	Molar ratios	
					SiO ₂	TiO ₂	Al ₂ O ₃	Fe ₂ O ₃	MgO	CaO	Na ₂ O	K ₂ O				Mg/Ca	Si/Ca
<i>Bedload</i>																	
BCT9	TSS	Nar	28.554	84.260	50.07	0.43	8.50	3.43	1.50	16.27	1.05	1.69	15.04	98.11		0.129	2.27
BCT10	TSS	Chame	28.552	84.241	38.03	0.42	7.00	2.90	1.74	23.55	0.72	1.60	21.32	97.36	0.71540	0.103	1.19
BCT39	TSS	Marsyandi	28.545	84.032	37.54	0.36	6.62	2.86	1.99	24.22	0.86	1.54	21.37	97.47	0.71441	0.115	1.14
BCT47	TSS + HHCS	Marsyandi	35.500	84.374											0.71969		
<i>Bedrock</i>																	
CR9	TSS	Limestone	28.687	83.997	59.04	0.67	12.26	7.58	1.78	6.67	1.83	1.48	7.98	99.45	0.71548	0.374	6.52
CR11	TSS	Quartzite	28.680	84.003											0.71477		
CR12	TSS	Black shale	28.678	84.003	52.02	1.46	32.86	0.70	0.11	0.12	1.51	6.93	4.81	100.56	0.71955	1.309	326
CR13	TSS	Psammite	28.680	84.003											0.72674		
CR14	TSS	Limestone	28.669	84.018	27.65	0.25	5.27	3.51	1.06	31.66	0.34	1.14	27.57	98.76		0.047	0.643
ett26R	TSS	Limestone	28.654	84.032	47.76	0.48	10.02	3.51	1.91	16.52	0.59	2.91	15.91	99.74	0.72051	0.161	2.131
ett43R	TSS	Limestone	28.777	83.977	7.43	0.17	1.76	1.54	4.99	43.08	0.00	0.16	38.12	97.31	0.70969	0.162	0.127
29b	HHCS	Calc-silicate	28.528	84.318	45.39	0.72	14.34	4.84	3.34	19.37	0.46	3.30	7.32	99.26	0.71649	0.242	1.73
ett113R	HHCS	Paragneiss	28.476	84.374	77.33	0.53	11.26	3.32	0.79	1.27	1.83	2.54	0.63	99.68	0.74912	0.292	31.5
ett127R	HHCS	Paragneiss	28.410	84.434	75.27	0.71	10.88	4.94	1.83	1.27	2.23	1.67	0.86	99.89	0.75940	0.673	30.6
<i>Leachates</i>																	
BCT10	TSS	1 h 5% acetic													0.71384	0.027	0.001
BCT10	TSS	10 min 5% acetic													0.71388	0.024	0.000
BCT10	TSS	1 h 10% acetic													0.71356	na	na
<i>Galy et al. (1999)</i>																	
<i>Leachates</i>																	
LO 315	Mixed														0.71306	0.057	0.003
NAG 22	TSS														0.71162	na	na
<i>Residues</i>																	
LO 315	Mixed														0.73658	4.159	79.7
NAG 22	TSS														0.72185	6.327	89.2

Major element data obtained by XRF, except for the leachate Si/Ca and Mg/Ca ratios which were determined by ICP-AES. BCT10 is the bedload from the Marsyandi at Chame, representative of the integrated output from the Marsyandi TSS. This sample was first leached in de-ionised water to remove loosely held Sr prior to cold acid leaching as indicated. Sample NAG22 from Galy et al. (1999) is from the headwaters of the Marsyandi, and LO315 is from the Marsyandi close to the confluence with the Trisuli.

6.2. Causes of seasonal variations in riverine chemistry

The variations in major ion concentration and $^{87}\text{Sr}/^{86}\text{Sr}$ ratios are consistent with a significant increase in the proportion of carbonate input to the dissolved load of Himalayan rivers during the monsoon. The most likely cause of this variation is the increased runoff from monsoonal precipitation and glacial meltwater which increases discharge by up to a factor of 12 (Sharma, 1997; Gabet et al., 2004). Seasonal variations in other parameters which may impact chemical weathering fluxes are less marked in the upper Marsyandi. For example, water temperatures only vary from 11.1 °C in April to 12.2 °C in September, a period which includes the most marked changes in river chemistry. Vegetation is sparse minimising potential biomass uptake (West et al., 2002).

The conclusion that discharge is the main control on compositional variability is supported by the close correspondence in short term variations in $\text{Si}(\text{OH})_4/\text{Ca}$ and

$^{87}\text{Sr}/^{86}\text{Sr}$ between the four rivers of the upper Marsyandi catchments (Fig. 3). Given that the four rivers drain spatially distinct catchments, the most probable common factor controlling such short term compositional variability is orographically enhanced storm events.

The variations in silicate and carbonate weathering fluxes from the Lirung catchment, where discharge data is available (Bhatt et al., 2000) provide further constraints on the causal relationships between weathering fluxes and runoff. This is not possible in the Marsyandi where published data is only available in the Lesser Himalaya where the important short-term variations in discharge are out of phase with the upper parts of the Marsyandi catchment.

Weathering fluxes are calculated as the product of discharge and carbonate or silicate ions partitioned using Eqs. (1) and (2). Runoff is estimated from the discharge and the catchment area. Many river systems exhibit a linear relationship with a zero intercept between weathering fluxes and runoff because the variations in chemical

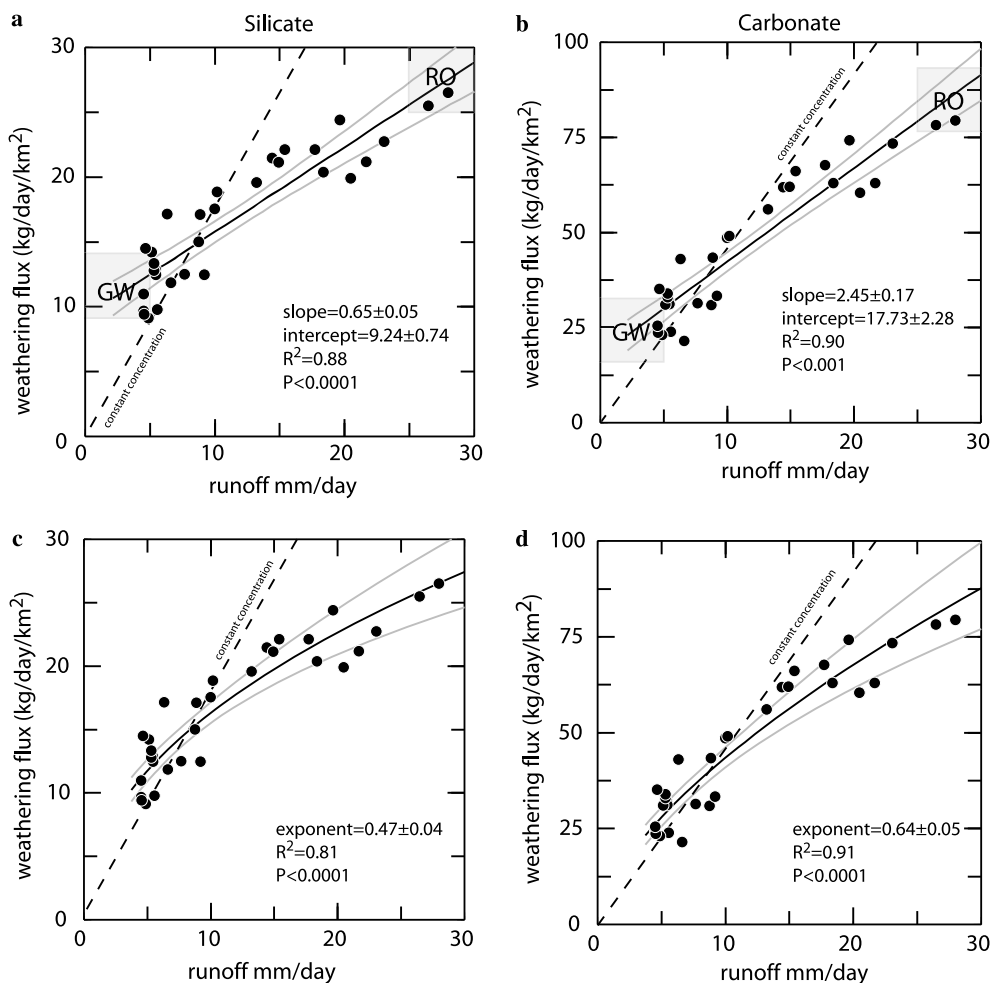


Fig. 7. The dependence of weathering flux on runoff for the Lirung catchment. Silicate Ca and Mg are estimated using Eqs. (1) and (2). Total silicate ions are the sum of Ca_{sil} , Mg_{sil} , K, and Na. Carbonate ions are estimated as total Ca and Mg less silicate Ca and Mg. GW is groundwater and RO is runoff, plotted schematically where they would be located (see text for discussion). (a) and (b) have been fitted with a straight line and (c) and (d) have been fitted by a power law relation. (solid lines with 1σ error bars). Dashed line is predicted for constant concentration plotted through the mean of the data. Note that the exponents in the power law fits are very similar to exponent of 0.65 used by Berner and Kothavala (2001) to model the dilution effects of weathering fluxes at a global scale.

concentrations are small compared with runoff (e.g. Bluth and Kump, 1994; Gaillardet et al., 1999). However, in the Lirung catchment (and the other Himalayan catchments discussed here), this is not so with a factor of 3 change in elemental concentration compared to a factor of 6 change in runoff. The data deviates significantly from the relationship between weathering flux and runoff where concentration remains constant (dashed lines, Fig. 7) or where a constant concentration weathering input is diluted or concentrated by an increase in runoff or evaporation (dashed lines, Fig. 8). The steeper slope for carbonate

merely reflects the greater concentration of carbonate ions.

The weathering flux–runoff data on Fig. 7 allow at least two explanations:

- (1) The trends are linear representing mixing of higher concentration component seen at low runoff with low concentration high runoff component, or
- (2) There is a non linear variation of concentration with runoff such that the data fit a power law relation (Figs. 7 c and d).

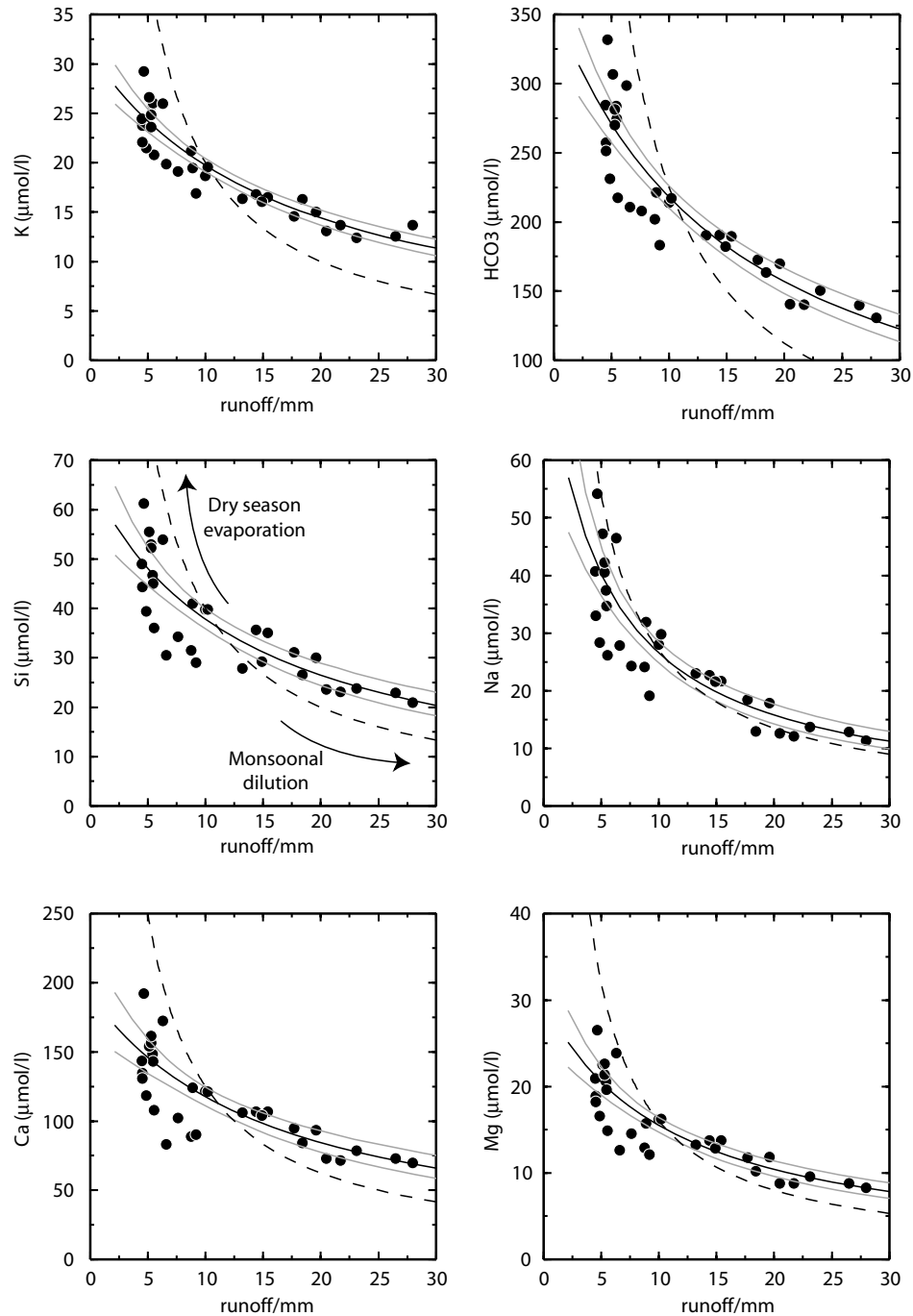


Fig. 8. Plots of concentration vs discharge for the Langtang. The dashed curves represent the effects of evaporation and dilution. The solid curves represent hyperbolic fits and error envelope (grey) to schematically illustrate the trends.

The single element-runoff relationships in Fig. 8 preclude a simple dilution-evaporation control and the consistent seasonal changes in $^{87}\text{Sr}/^{86}\text{Sr}$ ratios and elemental ratios (Figs. 3–5) in the Marsyandi strongly suggest that the water compositions are controlled by two-component mixing. Similar observations of high concentrations at low discharge and hence positive intercepts for chemical flux–runoff correlations (e.g. Bluth and Kump, 1994) have been explained by a groundwater discharge maintaining base flow augmented by more dilute water at high flow (e.g. White and Blum, 1995). These authors modelled evapotranspiration in a range of catchments and noted that recharge from groundwater was required to balance hydrological budgets in some catchments. Fairchild et al. (1999) report an increase in solute concentrations at low runoff in a similar Alpine environment, though cannot explain their data by a two component mixture between baseflow and rainwater. The importance of groundwater has been highlighted elsewhere in the world e.g. Anderson et al. (1997a,b), Ohruj and Mitchell (1999), Clauer et al. (2000), Johnson et al. (2000), and Rademacher et al. (2001) report that cation concentrations correlate with groundwater age, highlighting the importance of residence

time. The groundwater model for explaining the seasonal variations is illustrated schematically in Fig. 9 that the differing chemistries of the groundwater and rapid runoff components reflects control by dissolution kinetics and time available for mineral–water reactions. Carbonate dissolution is an order of magnitude faster than silicate (e.g. Alkattan et al., 1998; White et al., 1999; Welch and Ullman, 2000).

During the monsoon the contact time between the surface runoff and rock is short and the faster dissolution kinetics of carbonate allows a higher proportion of carbonate dissolution. Outside the monsoon, the rivers are fed mainly by shallow groundwater with the longer residence time allowing further dissolution of silicate whereas carbonate saturation is reached rapidly and limits further carbonate inputs. The observation that tributaries are saturated with respect to calcite even in the late monsoon (Table 1) attests to the relative rapidity of carbonate dissolution. Galy and France-Lanord (1999) and France-Lanord et al. (2003) have also reported that most Himalayan rivers are saturated with respect to calcite even in the monsoon.

The interpretation of the water compositions in the Himalayan catchments discussed here in terms of simple

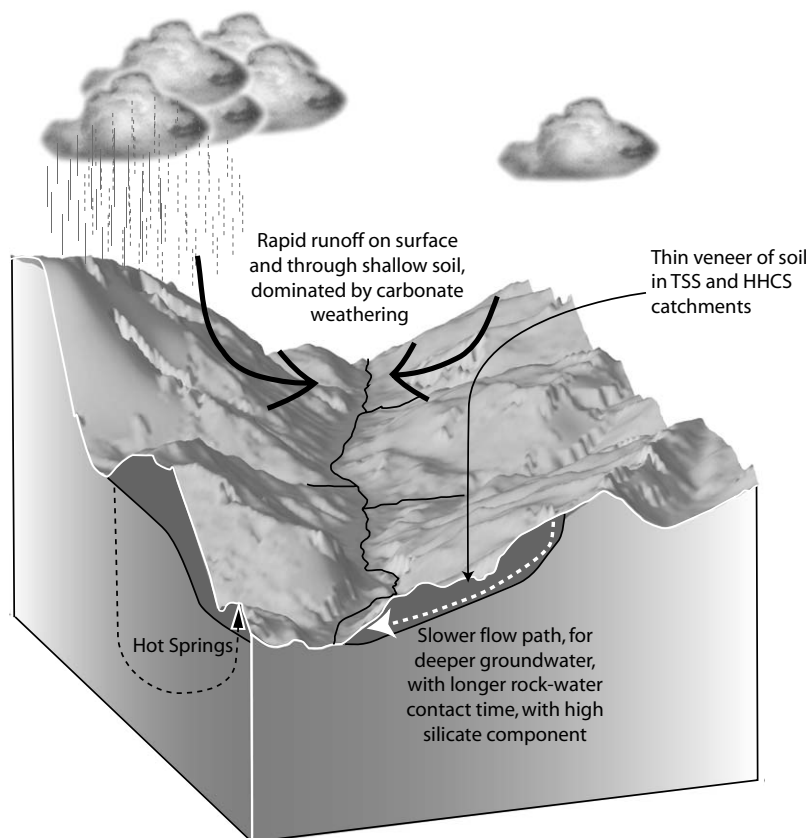


Fig. 9. Schematic of the potential sources of water to the Marsyandi. The faster dissolution kinetics of calcite means that it is more likely to respond rapidly to interaction with surface water whereas the slower dissolution kinetics of silicate minerals means that water with a longer water–rock interaction time will accumulate a larger fraction of ions from silicate weathering. In the winter when rainfall is low the base flow may be sourced from groundwater (Hendershot et al., 1992) with a higher proportion of silicate derived ions. In the summer discharge is dominated by monsoonal runoff with a greater proportion of carbonate derived ions. River waters may be affected by the hydrothermal springs reported by Evans et al. (2001, 2004) and Becker (2005) which have been corrected for in this study.

mixing between a groundwater and a rapid-runoff components is made with the knowledge that there are certainly other controls on the chemical weathering flux. These must include temperature (e.g. Velbel, 1993), biomass uptake (e.g. Drever, 1994) and freezing/melting cycles in the glaciated subcatchments (e.g. Anderson et al., 1997c; Fairchild et al., 1999) as well as potential complexities relating to variable groundwater paths and preferential exposure of fresh rock by landslides during the monsoon. The contrast in vegetation between the sparsely covered TSS and more densely forested HHCS may explain the observation that the compositional trends in the HHCS rivers are less prominent but demonstrates that vegetation does not mask the runoff control.

Despite the higher fraction of silicate weathering outside the monsoon, there is an overall increase in the silicate weathering flux during the monsoon in both the Lirung and Dokriani catchments. The monsoonal flux of silicate derived ions is approximately 60% of the total annual silicate weathering flux in each of the catchments. It is not possible to estimate the fluxes directly in the Marsyandi because there is no published discharge data. The monsoon silicate weathering flux has been estimated as a fraction of the total annual weathering flux by assuming that the upstream discharge scales directly with the published discharge (Fig. 2a) for the Marsyandi in the Lesser Himalaya (Sharma, 1997). This implies that the monsoonal silicate weathering flux is 50–70% of the total annual silicate weathering flux for the Marsyandi catchments.

7. Conclusions

The dissolved load in four rivers of the Marsyandi catchment (Nepal Himalaya) exhibit large seasonal variations in major cation ratios and Sr isotope ratios. A decrease in $\text{Si(OH)}_4/\text{Ca}$, X_{sil} , and Sr isotope ratios is consistent with a greater proportion of ions derived from carbonate weathering during the monsoon. The seasonal variations are not the result of changes in the location of precipitation, leading to runoff sampling distinct lithologies because the rivers in this study are small to medium catchments sampling relatively uniform lithology. The seasonal variations are even observed in first order tributaries, draining an area of several km^2 . The seasonal variations must reflect a differing response of carbonate and silicate lithologies to climatic forcing, and the strongly linear dependence of weathering flux on runoff confirms that runoff is the first order control. The faster dissolution kinetics of carbonate can explain why carbonate exhibits a greater sensitivity to runoff than silicate lithologies. At high runoff, the residence time of water is short, causing an increase in the proportion of carbonate to silicate derived ions. In contrast, in the dry season, the residence time of water is longer, permitting a greater proportion of silicate dissolution, relative to carbonate. There may be a greater proportion of silicate dissolution in groundwater where residence times are longer than surface water. In spite of the relative de-

crease in the silicate derived contribution to the dissolved load during the monsoon, the silicate weathering flux is dominated by the monsoonal flux, with 50–70% of the total silicate weathering flux occurring in the months June to September. Whilst the data presented here are relevant to annual time-scales the variations presented may provide insight to how the relative rates of silicate and carbonate weathering may change over longer time scales and particularly how weathering fluxes may have responded to climatic changes in runoff, a first order control on global chemical weathering fluxes.

Acknowledgments

This research has been supported by the Leverhulme Trust. Edward Tipper is supported by a NERC studentship No. NER/S/A/2002/10342. Katy Grant provided valuable support in the field. Fatima Khan performed a large portion of the Sr isotope chemistry. Mervyn Greeves provided assistance with ICP-AES. Ian Wilshaw at The University of Keele, Caroline Gorge from IPGP and Graham Howell from the OU are thanked for anion analysis. John Watson from the OU is thanked for XRF analysis. Tank P. Ohja provided valuable logistical assistance in Nepal. Doug Burbank is thanked for the infrastructure which made sampling possible on a weekly basis in the Marsyandi. J. Gaillardet, J. Drever, S. Krishnaswami (associate editor) and one anonymous reviewer are thanked for their thoughtful reviews and comments which substantially improved an earlier version of this manuscript.

Associate editor: S. Krishnaswami

References

- Alkattan, M., Oelkers, E.H., Dandurand, J.L., 1998. An experimental study of calcite and limestone dissolution rates as a function of pH from -1 to 3 and temperature from 25 to 80 °C. *Chem. Geol.* **151**, 199–214.
- Anderson, S.P., Dietrich, W.E., Montgomery, D.R., Torres, R., Conrad, M.E., Loague, K., 1997a. Subsurface flow paths in a steep, unchanneled catchment. *Water Resour. Res.* **33**, 2637–2653.
- Anderson, S.P., Dietrich, W.E., Torres, R., Montgomery, D.R., Loague, K., 1997b. Concentration–discharge relationships in runoff from a steep, unchanneled catchment. *Water Resour. Res.* **33**, 211–225.
- Anderson, S.P., Drever, J.I., Humphrey, N.F., 1997c. Chemical weathering in glacial environments. *Geology* **25**, 399–402.
- Becker, J.A., 2005. Quantification of Himalayan metamorphic CO₂ fluxes: Impact on global carbon budgets. Ph.D. Thesis, Dept. of Earth Sciences, University of Cambridge, Downing St., Cambridge, CB2 3EQ.
- Berner, R.A., Kothavala, Z., 2001. Geocarb III: a revised model of Atmospheric CO₂ over Phanerozoic time. *Am. J. Sci.* **301**, 182–204.
- Berner, R.A., Lasaga, A.C., Garrels, R.M., 1983. The carbonate–silicate geochemical cycle and its effect on atmospheric carbon dioxide over the past 100 million years. *Am. J. Sci.* **283**, 641–683.
- Bhatt, M.P., Masuzawa, T., Yamamoto, M., Sakai, A., Fujita, K., 2000. Seasonal changes in dissolved chemical composition and flux of meltwater draining from Lirung Glacier in the Nepal Himalayas. In: Nakawo, M. (Ed.), *Debris-Covered Glaciers: IAHS Publication 264*, pp. 277–288.

- Bickle, M.J., Bunbury, J., Chapman, H.J., Harris, N.B.W., Fairchild, I., Ahmad, T., 2001. Controls on the Sr ratio of Carbonates in the Garhwal Himalaya, Headwaters of the Ganges. *J. Geol.* **109**, 737–753.
- Bickle, M.J., Bunbury, J., Chapman, H.J., Harris, N.B.W., Fairchild, I., Ahmad, T., 2003. Fluxes of Sr into the Headwaters of the Ganges. *Geochim. Cosmochim. Acta* **67**, 2567–2584.
- Bickle, M.J., Chapman, H.J., Bunbury, J., Harris, N.B.W., Fairchild, I.J., Ahmad, T., Pomiès, C., 2005. Relative contributions of silicate and carbonate rocks to riverine Sr fluxes in the headwaters of the Ganges. *Geochim. Cosmochim. Acta* **69**, 2221–2240.
- Blum, J.D., Carey, A.G., Jacobson, A.D., Chamberlain, P., 1998. Carbonate versus silicate weathering in the Raikhot watershed within the High Himalayan Crystalline Series. *Geology* **26**, 411–414.
- Bluth, G.J., Kump, L.R., 1994. Lithologic and climatologic controls of river chemistry. *Geochim. Cosmochim. Acta* **58**, 2341–2359.
- Bookhagen, B., Thiede, R.C., Strecker, M.R., 2005. Abnormal monsoon years and their control on erosion and sediment flux in the High, arid and northwest Himalaya. *Earth Planet. Sci. Lett.* **231**, 131–146.
- Bordet, P., Colchen, M., Krummenacher, D., Lefort, P., Mouterde, R., Remy, M., 1971. *Recherches Géologiques dans l'Himalaya du Nepal region de la Thakkhola*. Editions du centre national de la recherche scientifique.
- Burbank, D., Blythe, A., Putkonen, J., Pratt-Sitaula, B., Gabet, E., Oskin, M., Barros, A., Ojha, T., 2003. Decoupling of erosion and precipitation in the Himalayas. *Nature* **426**, 652–655.
- Clauer, N., Chaudhuri, S., Toulkeridis, T., Blanc, G., 2000. Fluctuations of Caspian Sea level: beyond climatic variations? *Geology* **28**, 1015–1018.
- Colchen, M., Le Fort, P., Pecher, A., 1986. *Notice explicative de la Carte Géologique Annapurna–Manaslu–Ganesh (Himalaya du Nepal) au 1:200.000e*. Centre National de la recherche Scientifique.
- Coleman, M., 1996. Orogen-parallel and orogen-perpendicular extension in the central Nepalese Himalayas. *Geol. Soc. Am. Bull.* **108**, 1594–1607.
- Dalai, T.K., Bhattacharya, S., Krishnaswami, S., 2002a. Stable isotopes in the source waters of the Yamuna and its tributaries: seasonal and altitudinal variations and relation to major cations. *Hydrol. Process.* **16**, 3345–3364.
- Dalai, T.K., Krishnaswami, S., Kumar, A., 2003. Sr and $^{87}\text{Sr}/^{86}\text{Sr}$ in the Yamuna River System in the Himalaya: sources, fluxes, and controls on Sr isotope composition. *Geochim. Cosmochim. Acta* **67**, 2931–2948.
- Dalai, T.K., Krishnaswami, S., Sarin, M.M., 2002b. Major ion chemistry in the headwaters of the Yamuna river system: chemical weathering, its temperature dependence and CO_2 consumption in the Himalaya. *Geochim. Cosmochim. Acta* **66**, 3397–3416.
- Dessert, C., Dupré, B., Francois, L.M., Schott, J., Gaillardet, J., Chakrapani, G., Bajpai, S., 2001. Erosion of Deccan Traps determined by river geochemistry: impact on the global climate and the $^{87}\text{Sr}/^{86}\text{Sr}$ ratio of seawater. *Earth Planet. Sci. Lett.* **188**, 459–474.
- Drever, J.I., 1994. The effect of land plants on weathering rates of silicate minerals. *Geochim. Cosmochim. Acta* **58**, 2325–2332.
- Edmond, J.M., 1992. Himalayan tectonics, weathering processes, and the strontium isotope record in marine limestones. *Science* **258**, 1594–1597.
- English, N., Quade, J., DeCelles, P., Garzzone, C., 2000. Geologic control of Sr and major element chemistry in Himalayan Rivers, Nepal. *Geochim. Cosmochim. Acta* **64**, 2549–2566.
- Evans, M.J., Derry, L.A., Anderson, S., France-Lanord, C., 2001. Hydrothermal source of radiogenic Sr to Himalayan rivers. *Geology* **29**, 803–806.
- Evans, M.J., Derry, L.A., France-Lanord, C., 2004. Geothermal fluxes of alkalinity in the Narayani river system of central Nepal. *Geochem. Geophys. Geosyst.* **5**, Q08011.
- Fairchild, I.J., Killawee, J.A., Sharp, M.J., Spiro, B., Hubbard, B., Lorrain, R.D., Tison, J.L., 1999. Solute generation and transfer from a chemically reactive alpine glacial-proglacial system. *Earth Surf. Process. Landf.* **24**, 1189–1211.
- France-Lanord, C., Derry, L., Michard, A., 1993. Evolution of the Himalayan since Miocene time, isotopic and sedimentological evidence from the Bengal fan. *Geol. Soc. London Spec. Publ.* **74**, 603–621.
- France-Lanord, C., Evans, M., Hurtrez, J.E., Riotte, J., 2003. Annual dissolved fluxes from Central Nepal rivers: budget of chemical erosion in the Himalayas. *CR Geosci.* **335**, 1131–1140.
- Gabet, E.J., Burbank, D.W., Putkonen, J.K., Pratt-Sitaula, B.A., Ojha, T., 2004. Rainfall thresholds for landsliding in the Himalayas of Nepal. *Geomorphology* **63**, 131–143.
- Gaillardet, J., Dupré, B., Louvat, P., Allegre, C.J., 1999. Global silicate weathering and CO_2 consumption rates deduced from the chemistry of large rivers. *Chem. Geol.* **159**, 3–30.
- Galy, A., France-Lanord, C., 1999. Weathering processes in the Ganges-Brahmaputra basin and the riverine alkalinity budget. *Chem. Geol.* **159**, 31–60.
- Galy, A., France-Lanord, C., Derry, L.A., 1999. The strontium isotopic budget of Himalayan Rivers in Nepal and Bangladesh. *Geochim. Cosmochim. Acta* **63**, 1905–1925.
- Garrels, R., Mackenzie, F., 1967. Origin of the chemical compositions of some springs and lakes. *Am. Chem. Soc.: Adv. Chem. Ser.* **67**, 222–242.
- Gibbs, M.T., Kump, L.R., 1994. Global chemical erosion during the last glacial maximum and the present: sensitivity to changes in lithology and hydrology. *Paleoceanography* **9**, 529–544.
- Harris, N., Bickle, M.J., Chapman, H., Fairchild, I., Bunbury, J., 1998. The significance of Himalayan rivers for silicate weathering rates: evidence from the Bhote Kosi tributary. *Chem. Geol.* **144**, 205–220.
- Hasnain, S.I., Thayyen, R.J., 1999. Controls on the major-ion chemistry of the Dokriani glacier meltwaters, Ganga basin, Garhwal Himalaya, India. *J. Glaciol.* **45**, 87–92.
- Hendershot, W., Savoie, S., Courchesne, F., 1992. Simulation of stream-water chemistry with soil solution and groundwater flow contributions. *J. Hydrol.* **136**, 237–252.
- Holmes, J.A., 1996. Trace-element and stable-isotope geochemistry of non-marine ostracod shells in Quaternary palaeoenvironmental reconstruction. *J. Paleolimnol.* **15**, 223–235.
- Jacobson, A.D., Blum, J.D., 2000. Ca/Sr and $^{87}\text{Sr}/^{86}\text{Sr}$ geochemistry of disseminated calcite in Himalayan silicate rocks from the Naga Parbat: influence on river water chemistry. *Geology* **28**, 463–466.
- Jacobson, A.D., Blum, J.D., Chamberlain, C.P., Craw, D., Koons, P.O., 2003. Climatic and tectonic controls on chemical weathering in the New Zealand Southern Alps. *Geochim. Cosmochim. Acta* **67**, 29–46.
- Jacobson, A.D., Blum, J.D., Walter, L.M., 2002. Reconciling the elemental and Sr isotope composition of Himalayan weathering fluxes: insights from the carbonate geochemistry of stream waters. *Geochim. Cosmochim. Acta* **66**, 3417–3429.
- Johnson, T.M., Roback, R.C., McLing, T.L., Bullen, T.D., DePaolo, D.J., Doughty, C., Hunt, R.J., Smith, R.W., Cecil, L.D., Murrell, M.T., 2000. Groundwater fast paths in the Snake River Plain aquifer: radiogenic isotope ratios as natural groundwater tracers. *Geology* **28**, 871–874.
- Karim, A., Veizer, J., 2000. Weathering processes in the Indus River Basin: implications from riverine carbon, sulphur, oxygen and strontium isotopes. *Chem. Geol.* **170**, 153–177.
- Krishnaswami, S., Singh, S., Dalai, T., 1999. Silicate weathering in the Himalaya: role in contributing to major ions and radiogenic Sr to the Bay of Bengal. In: Somayajulu, B.L.K. (Ed.), *Ocean Science, Trends and Future Directions*. Indian National Science Academy and Akademia International, New Delhi, pp. 23–51.
- Krishnaswami, S., Trivedi, J., Sarin, M., Ramesh, R., Sharma, K., 1992. Strontium isotopes and rubidium in the Ganga-Brahmaputra river system: weathering in the Himalaya, fluxes to the Bay of Bengal and contributions to the evolution of oceanic Sr. *Earth Planet. Sci. Lett.* **109**, 243–253.
- Le Fort, P., 1975. Himalayas, the collided range, present knowledge of the continental arc. *Am. J. Sci.* **275A**, 1–44.
- Negrel, P., Allegre, C.J., Dupré, B., Lewin, E., 1993. Erosion sources determined by inversion of major and trace elements ratios and

- strontium isotopic ratios in river water: the Congo Basin Case. *Earth Planet. Sci. Lett.* **120**, 59–76.
- Ohruai, K., Mitchell, M., 1999. Hydrological flow paths controlling stream chemistry in Japanese forested watersheds. *Hydrol. Process.* **13**, 877–888.
- Oliver, L., Harris, N., Bickle, M., Chapman, H., Dise, N., Horstwood, M., 2003. Silicate weathering rates decoupled from the ^{87}Sr ratio of the dissolved load during Himalayan erosion. *Chem. Geol.* **201**, 119–139.
- Palmer, M.R., Edmond, J.M., 1992. Controls over the strontium isotope composition of river water. *Earth Planet. Sci. Lett.* **56**, 2099–2111.
- Pande, K., Sarin, M., Trivedi, J., Krishnaswami, S., Sharma, K., 1994. The Indus River system (India–Pakistan): major-ion chemistry, uranium and Sr isotopes. *Chem. Geol.* **116**, 245–259.
- Quade, J., English, N., DeCelles, P.G., 2003. Silicate versus carbonate weathering in the Himalaya: a comparison of the Arun and Seti River watersheds. *Chem. Geol.* **202**, 276–296.
- Quade, J., Roe, L., DeCelles, P.G., Ojha, T.P., 1997. The late Neogene $^{87}\text{Sr}/^{86}\text{Sr}$ record of lowland Himalayan rivers. *Science* **276**, 1826.
- Rademacher, L.K., Clark, J.F., Hudson, G.B., Erman, D.C., Erman, N.A., 2001. Chemical evolution of shallow groundwater as recorded by spring, Sagehen basin; Nevada County, California. *Chem. Geol.* **179**, 37–51.
- Ramsey, M., Potts, P., Webb, P., Watkins, P., Watson, J., Coles, B., 1995. An objective assessment of analytical method precision—comparison of ICP-AES and XRF for the analysis of silicate rocks. *Chem. Geol.* **124**, 1–19.
- Raymo, M.E., 1994. The Himalayas, organic carbon burial, and climate in the Miocene. *Paleoceanogr. currents* **9**, 399–404.
- Richter, F.M., Rowley, D.B., DePaolo, D.J., 1992. Sr isotope evolution of seawater: the role of tectonics. *Earth Planet. Sci. Lett.* **109**, 11–23.
- Riebe, C.S., Kirchner, J.W., Granger, D.E., Finkel, R.C., 2001. Strong tectonic and weak climatic control of long-term chemical weathering rates. *Geology* **29**, 511–514.
- Sarin, M.M., Krishnaswami, S., Dilli, K., Somayajulu, B.L., Moore, W.S., 1989. Major ion chemistry of the Ganga–Brahmaputra river system: Weathering processes and fluxes to the Bay of Bengal. *Geochim. Cosmochim. Acta* **53**, 997–1009.
- Searle, M.P., Godin, L., 2002. The South Tibetan Detachment Zone and the Manaslu Leucogranite: a structural reinterpretation and restoration of the Annapurna–Manaslu Himalaya, Nepal. *J. Geol.* **111**, 505–523.
- Sharma, C.K., 1997. *A Treatise on Water Resources of Nepal*. Sangeeta Sharma, Kathmandu, p. 493.
- Singh, S.K., Sarin, M.M., France-Lanord, C., 2005. Chemical erosion in the eastern Himalaya: major ion composition of the Brahmaputra and $\delta^{13}\text{C}$ of dissolved inorganic carbon. *Geochim. Cosmochim. Acta* **69**, 3573–3588.
- Singh, S.K., Trivedi, J.R., Pande, K., Ramesh, R., Krishnaswami, S., 1998. Chemical and strontium, oxygen, and carbon isotopic compositions of carbonates from the Lesser Himalaya: implications to the strontium isotope composition of the source waters of the Ganga, Ghaghara, and the Indus rivers. *Geochim. Cosmochim. Acta* **62**, 743–755.
- Stallard, R.F., 1995. Relating chemical and physical erosion. *Rev. Min. Geochem.* **31**, 543–564.
- Stewart, B.W., Capo, R.C., Chadwick, O.A., 1998. Quantitative strontium isotope models for weathering, pedogenesis and biogeochemical cycling. *Geoderma* **82**, 173–195.
- Sundquist, E.T., 1991. Steady-and-non-steady-state carbonate–silicate controls on atmospheric CO_2 . *Quat. Sci. Rev.* **10**, 283–296.
- Tesoriero, A.J., Pankow, J.F., 1996. Solid solution partitioning of Sr^{2+} , Ba^{2+} , and Cd^{2+} to calcite. *Geochim. Cosmochim. Acta* **60**, 1053–1063.
- Velbel, M., 1993. Temperature dependence of silicate weathering in nature: How strong a negative feedback on long term accumulation of atmospheric CO_2 and global greenhouse warming? *Geology* **21**, 1059–1062.
- Walker, J.C.G., Hays, P.B., Kasting, J.F., 1981. A negative feedback mechanism for the long-term stabilization of Earth's surface temperature. *J. Geophys. Res.* **86**, 9776–9782.
- Welch, S.A., Ullman, W.J., 2000. The temperature dependence of bytownite feldspar dissolution in natural aqueous solutions of inorganic and organic ligands at low temperatures (5–35 °C). *Chem. Geol.* **167**, 337–354.
- West, A.J., Bickle, M.J., Collins, R., Brasington, J., 2002. Small-catchment perspective on Himalayan weathering fluxes. *Geology* **30**, 355–358.
- West, A.J., Galy, A., Bickle, M., 2005. Tectonic and climatic controls on silicate weathering. *Earth Planet. Sci. Lett.* **235**, 211–228.
- White, A.F., Blum, A.E., 1995. Effects of climate on chemical weathering in watersheds. *Geochim. Cosmochim. Acta* **59**, 1729.
- White, A.F., Blum, A.E., Schultz, M.S., Vivit, D.V., Stonestrom, D.A., Larson, M., Murphy, S.F., Eberl, D., 1998. Chemical weathering in a tropical watershed, Luquillo Mountains, Puerto Rico: I. Long-term versus short term weathering fluxes. *Geochim. Cosmochim. Acta* **62**, 209–226.
- White, A.F., Bullen, T.D., Vivit, D.V., 1999. The role of disseminated calcite in the chemical weathering of granitoid rocks. *Geochim. Cosmochim. Acta* **63**, 1939–1953.